

Fully murine CD105-targeted CAR-T cells provide an immunocompetent model for CAR-T cell biology

Konstantinos Lontos^{a,b}, Yiyang Wang^c, Mason Colbert^a, Alok Kumar^a, Supriya Joshi^a, Mary Philbin^a, Yupeng Wang^{a,c}, Andrew Frisch^{a,d}, Jason Lohmueller^e, Dayana B. Rivadeneira^a, and Greg M. Delgoffe^a

^aTumor Microenvironment Center, Department of Immunology, UPMC Hillman Cancer Center and University of Pittsburgh, Pittsburgh, PA, USA; ^bDivision of Hematology/Oncology, UPMC, Pittsburgh, PA, USA; ^cSchool of Medicine, Tsinghua University, Beijing, Peking, China; ^dGraduate Program of Microbiology and Immunology, University of Pittsburgh School of Medicine, Pittsburgh, PA, USA; ^eDepartment of Surgery, Hillman Cancer Center, University of Pittsburgh, Pittsburgh, PA, USA

ABSTRACT

The modeling of chimeric antigen receptor (CAR) T cell therapies has been mostly focused on immunodeficient models. However, there are many advantages in studying CAR-T cell biology in an immunocompetent setting. We generated a fully murine CAR targeting CD105 (endoglin), a component of the TGF β receptor expressed on the surface of certain solid tumors and acute leukemias. CD105-targeted CAR-T cells can be grown from various murine backgrounds, tracked *in vivo* by congenic marks, and be activated by CD105 in isolation or expressed by tumor cells. CD105-targeted CAR-T cells were toxic at higher doses but proved safe in lower doses and modestly effective in treating wild-type B16 melanoma-bearing mice. CAR-T cells infiltrating the tumor expressed high levels of exhaustion markers and exhibited metabolic insufficiencies. We also generated a human CD105 CAR, which was efficacious in treating human melanoma and acute myeloid leukemia *in vivo*. Our work details a new murine model of CAR-T cell therapy that can be used from immunologists to further our understanding of CAR-T cell biology. We also set the foundation for further exploration of CD105 as a possible human CAR-T cell target.

ARTICLE HISTORY

Received 29 June 2022
Revised 27 September 2022
Accepted 28 September 2022

KEYWORDS

cd105; B16; murine CAR-T cell; immunocompetent CAR-T; AML; acute myeloid leukemia; CD105 CAR-T cell

Introduction

Years of foundational work by cancer immunologists culminated in recognition of cancer immunotherapy as the fourth pillar of cancer treatment in 2013.¹ This recognition came after the advent of checkpoint blockade, which drastically changed the treatment landscape of many malignancies.² In addition to checkpoint blockade, the FDA approved chimeric antigen receptor (CAR) T cells in 2017, paving the road for cure in patients with refractory B cell malignancies.³


CAR-T cells are T cells isolated from patients and engineered through a variety of techniques (ie retroviral transduction, lentiviral transduction or other methods) to express a CAR. The CAR has a single-chain variable fragment (scFv) that binds to an antigen such as CD19. Following transduction, the cells are re-infused in the patient.³ After binding, the receptor activates the T cell through the CD3 ζ domain and a costimulatory domain, typically 4-1BB or CD28, ultimately leading to activation and target cell death. CAR-T cells have exhibited high and sustained responses in patients with B cell malignancies and myeloma leading to FDA approval for multiple indications.⁴⁻⁶ However, some cases of acute lymphoblastic leukemia will eventually relapse, and half of the patients with diffuse large B-cell lymphoma will see their disease progress quickly after treatment.^{7,8} Furthermore, the results

of CAR-T cell therapy against solid tumor malignancies have been so far disappointing.⁹

To further improve on our current CAR-T cell armamentarium we need efficient and representative modeling. Unfortunately, preclinical modeling of human CAR-T cells is expensive and laborious. The 'gold standard' approaches generally utilize NOD.scid.il2rg (NSG) mice bearing tumors generally derived from cell lines, and typically the transfer of non-MHC matched CAR-T cells. While these CAR-T cells can recognize tumor antigen *in vivo* and mediate tumor killing, they also can mediate allogeneic responses to the tumor and xenogeneic responses to murine tissues, ultimately resulting in GVHD. In addition, the NSG model does not allow us to study CAR-T cells in an immunocompetent environment and precludes *in vivo* stimulation of these cells from healthy tissue antigens. An important solution to this problem that could complement the NSG model is fully murine CAR-T cells targeting a naturally occurring tumor surface antigen. However, this avenue has only been explored for very few targets in the purview of biotech industry.¹⁰⁻¹⁶

In this study, we detail the identification, design, and engineering of a fully murine CAR targeting CD105, a cell surface receptor typically expressed by activated endothelium but highly overexpressed on a broad array of tumor types including melanoma and acute myelogenous leukemia

CONTACT Greg M. Delgoffe  delgoffe@upmc.edu  Tumor Microenvironment Center, Department of Immunology, UPMC Hillman Cancer Center and University of Pittsburgh, 5117 Centre Avenue, 2.26b HCC, Pittsburgh, PA, USA

 Supplemental data for this article can be accessed online at <https://doi.org/10.1080/2162402X.2022.2131229>

© 2022 The Author(s). Published with license by Taylor & Francis Group, LLC.

This is an Open Access article distributed under the terms of the Creative Commons Attribution-NonCommercial License (<http://creativecommons.org/licenses/by-nc/4.0/>), which permits unrestricted non-commercial use, distribution, and reproduction in any medium, provided the original work is properly cited.

(AML).^{17,18} We show this murine CAR produces all of the ‘problems’ associated with CAR-T cells: despite remarkable killing efficiency *in vitro*, CD105 CAR-T cells are weakly effective *in vivo* and carry the potential for toxicity. This fully murine CAR-T system can be used to identify regulatory mechanisms and reprogramming strategies that will broadly enable cellular therapies for cancer. Further, we demonstrate feasibility of creating human CAR-T cells targeting CD105 based off an antibody already in use for clinical trials.

Results

CD105 is a Surface Target on B16 Melanoma Targetable With Murine CAR-T Cells

As there are no available fully murine CAR-T cell models that directly target B16 melanoma, the widely used tumor model used in immunology research, we sought to find a suitable target. Consistent with other groups, we found high endoglin (CD105) expression in B16 melanoma (Figure 1a). We investigated further the B16 tumor

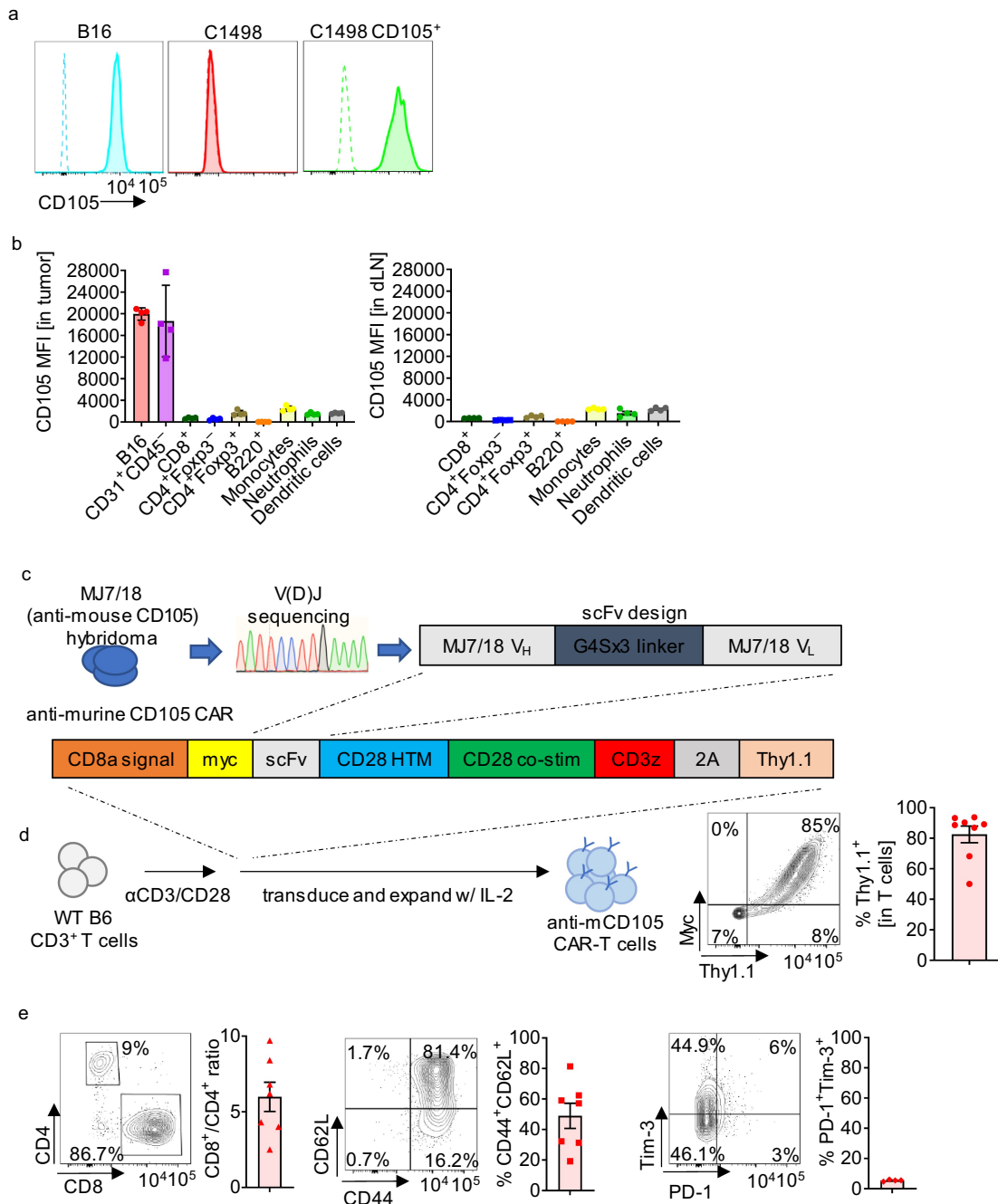


Figure 1. Generation of a fully murine chimeric antigen receptor (CAR) to CD105, a natural murine tumor surface target. (a) CD105 expression of B16 & C1498 (b) Comparison of CD105 expression in the B16 microenvironment and the lymph nodes (c) Schematic of engineering of the fully murine CD105-targeted CAR (d) Schema of murine CAR-T cell generation using a retroviral expression construct in C. Thy1.1 and Myc staining are shown confirming transduction and surface expression of the CD105-specific CAR. (e) Flow cytometric analysis of the murine CD105-targeted CAR product at the end of expansion (day 7). The data in figure (b) are from one experiment which included four different mice, each with one B16 tumor. Each point on D, E represents expansion of CAR-T cells from a different mouse donor.

infiltrate for expression of CD105. CD105 expression was retained in B16 cells *in vivo* and was also highly expressed in activated tumor vasculature (Figure 1b). In contrast, it was undetectably or modestly expressed in most hematopoietic cells in the tumor or lymph nodes (Figure 1b). Given that CD105 has also been targeted in mice with a monoclonal antibody without toxicities,¹⁹ we engineered a CAR against CD105. We sequenced the variable heavy- and light-chain regions of the MJ7/18 hybridoma and constructed a single chain variable fragment (scFv) which we inserted in a MSGV-based retroviral backbone consisting of murine hinge and transmembrane (HTM) CD28 domain, followed by murine CD28 costimulatory and murine CD3z domain as previously reported in a murine CD19-targeted CAR (Figure 1c).¹⁰ The murine CD3z domain has all three immunoreceptor tyrosine-based activation motifs (ITAMs) intact. We added a myc tag on the N-terminus of the CAR and a Thy1.1 bicistronic tag to the construct to facilitate detection of cell surface expression and transduction, respectively. Transduction with this construct in bulk murine C57/BL6J T cells led to consistently high expression of the CAR (Figure 1d). At the end of expansion (day 7 from activation) the murine CD105-targeted CAR-T cells consisted mainly of CD8⁺ central memory (CD44⁺CD62L⁺) T cells and expressed low levels of inhibitory receptors (Figure 1e). The low expression of inhibitory receptors are indicative of low levels of tonic signaling.

Murine CD105 CAR-T Cells are Active Against CD105⁺ Tumors

Next, we investigated whether this murine CAR signaled and functioned appropriately. Murine CD105-directed CAR-T cells were activated by the plate-bound CD105 but not by PBS as evidenced by upregulation of CD44, CD69, CD25 and downregulation of CD62L (Figure 2a). In addition, they produced high amounts of cytokines (IFN- γ , TNF- α , Granzyme B, IL-2) (Figure 2b) and initiated proliferation (Figure 2c). Mock-transduced T cells were not activated by plate-bound CD105 or PBS, demonstrating specificity for CD105 reactivity. Next, we sought to investigate if the murine CAR can be activated by antigen-expressing tumors. Indeed, after overnight incubation with B16-F10, which expresses high levels of CD105 at steady state, CAR-T cells were activated (Figure 2d) and actively producing cytokines (Figure 2d). To explore the specificity of the CAR function, we employed a murine leukemia cell line (C1498) that lacks CD105 expression at baseline, and a variant of this line that we transduced with CD105 (Figure 1a). Co-culture of murine CD105-targeted CAR-T cells with either the wild-type C1498 or CD105-overexpressing C1498 cell line revealed activation only by the cell line expressing CD105, confirming the specificity of the CAR (Figure 2e and f). Finally, we examined the killing capacity of the murine CD105-targeted CD105 CAR utilizing luciferase killing assays. The murine CD105-targeted CAR-T cells killed B16 and C1498 CD105⁺ *in vitro* but exhibited no killing capacity against wild-type (CD105⁻) C1498 (Figure 2g).

High Doses of Murine CD105 CAR-T Cells Induce Toxicity in the Lymphodepleted Setting

We next sought to determine the efficacy of CD105-targeted murine CAR-T cells *in vivo*. Initially, we injected 3 million CD105-targeted murine CAR-T cells without prior conditioning, observing no toxicity in the mice (Figure 3a). However, most patients receive lymphodepletion before their CAR-T cell infusion to aid engraftment. Thus, we repeated the experiment with cyclophosphamide pre-conditioning (Figure 3b), which led to rapid weight loss (Figure 3c). Analysis of serum cytokines two days after CAR-T cell injection revealed a profound increase in many inflammatory and type I cytokines, consistent with a cytokine storm (Figure 3d). In addition, a necropsy performed after sacrificing the mice due to morbidity showed lymphocytic infiltrates around vessels in the lungs and the liver (Figure 3e). No other lesions were observed. We followed-up this finding with immunofluorescence of healthy lung and liver tissue and we found expression of CD105 on healthy vessels (Figure 3f). This finding was not consistent with previous literature, which suggested that CD105 is only present in activated vasculature, although this claim has been mostly investigating in humans.²⁰ In our effort to reduce the toxicity observed in the mice we performed a dose titration and we showed that by decreasing the CAR-T cell dose to 500,000 cells, we were able to rescue the mice from toxicity (Figure 3g). To confirm that the absence of toxicity was not because of minimal engraftment due to the lower T cell dose we assayed the blood of the mice 14 days after CAR-T cell infusion. The cohort that received the lower dose of murine CAR-T cells after cyclophosphamide had significant engraftment, consisting of about 16–20% of all CD45⁺ circulating cells (Figure 3h). We assayed this engraftment serially up to day 50 post-infusion and we found that it remained stable (Sup. Figure 1A).

CD105-Targeted Murine CAR-T Cells are Active Against B16 Melanoma *in vivo*

Next, we evaluated the efficacy of the CD105-targeted murine CAR-T cells. We injected B16 melanoma-bearing C57BL/6 mice with 500,000 CAR-T cells after lymphodepletion (Figure 4a) and we observed a significant reduction in tumor growth which resulted in doubling of survival (Figure 4b). Of note, when we performed the same experiment using 3 million CD8 HTM/4-1BB co-stimulatory domain mouse CAR-T cells we observed no toxicity, but no efficacy as has happened in prior literature (Sup. Figure 1B).¹⁴ As the tumors were not cleared from the CD28-based CAR-T cells, we sought to investigate potential underlying mechanisms, including lowered persistence, ineffective infiltration, T cell intrinsic dysfunction (exhaustion), and impaired signaling of the CAR. We analyzed the tumor-infiltrating leukocytes (TIL) of intradermal B16 tumors 14 days after injection. First, the transferred CAR-T cells were the predominant T lymphocyte found inside the tumor, ruling out impaired trafficking to the tumor (Figure 4c). Despite the CAR-T cells being predominantly (~90%) CD8⁺ on injection, the infiltrate in the lymph node had equal amounts of CD4⁺ and CD8⁺ CAR⁺ T cells, whereas the tumor harbored mainly CD8⁺ CAR-T cells (Figure 4d).

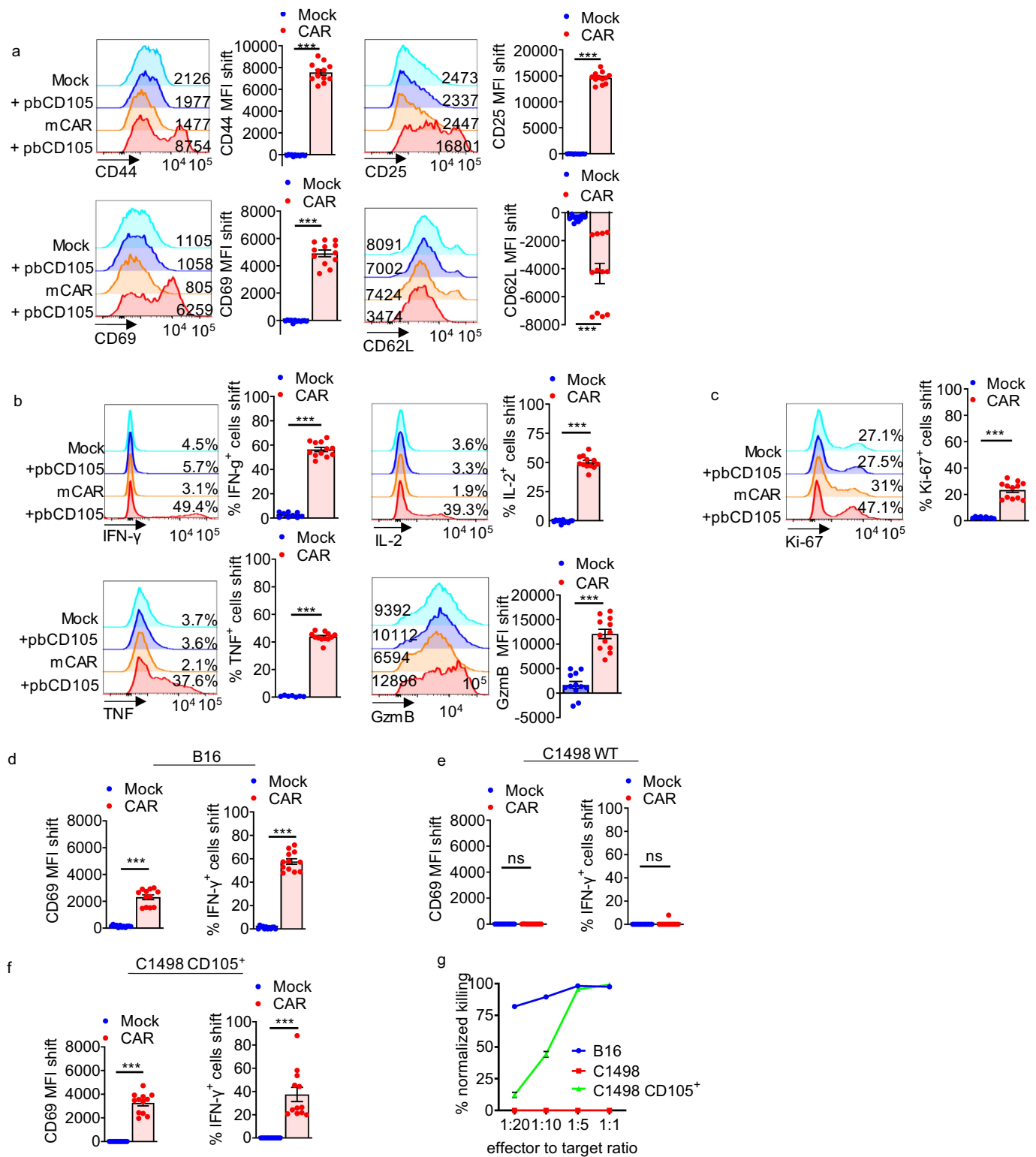


Figure 2. Murine CD105-targeted CAR-T cells are activated through CD105 and exhibit CD105-dependent killing activity. (a) Surface activation markers after overnight incubation of the murine CAR-T cells with 2 ug/ml of plate-bound CD105 (pbCD105). (b) Intracellular cytokines after overnight incubation of the murine CAR-T cells with 2 ug/ml plate-bound CD105. (c) Ki-67 expression after overnight incubation of the murine CAR-T cells with 2 ug/ml plate-bound CD105. (d) Activation markers after overnight incubation of murine CAR-T cells with B16 melanoma at 1:1 ratio. (e) Activation markers after overnight incubation of murine CAR-T cells with wild-type C1498 murine leukemia at 1:1 ratio. (f) Activation markers after overnight incubation of murine CAR-T cells with CD105⁺ C1498 murine leukemia at 1:1 ratio. (g) Luciferase killing assays after overnight incubation of murine CAR-T cells with target cell lines, normalized to the mock-transduced killing activity. All experiments were repeated with 3 different mouse donors and data from these experiments were pooled. MFI shift was defined as MFI of T cells co-incubated with target cell lines minus MFI of cells in regular culture conditions. Statistics are either unpaired t-test or Wilcoxon rank sum test depending on the observed data distribution. * $p < .05$, ** $p < .01$, *** $p < .001$.

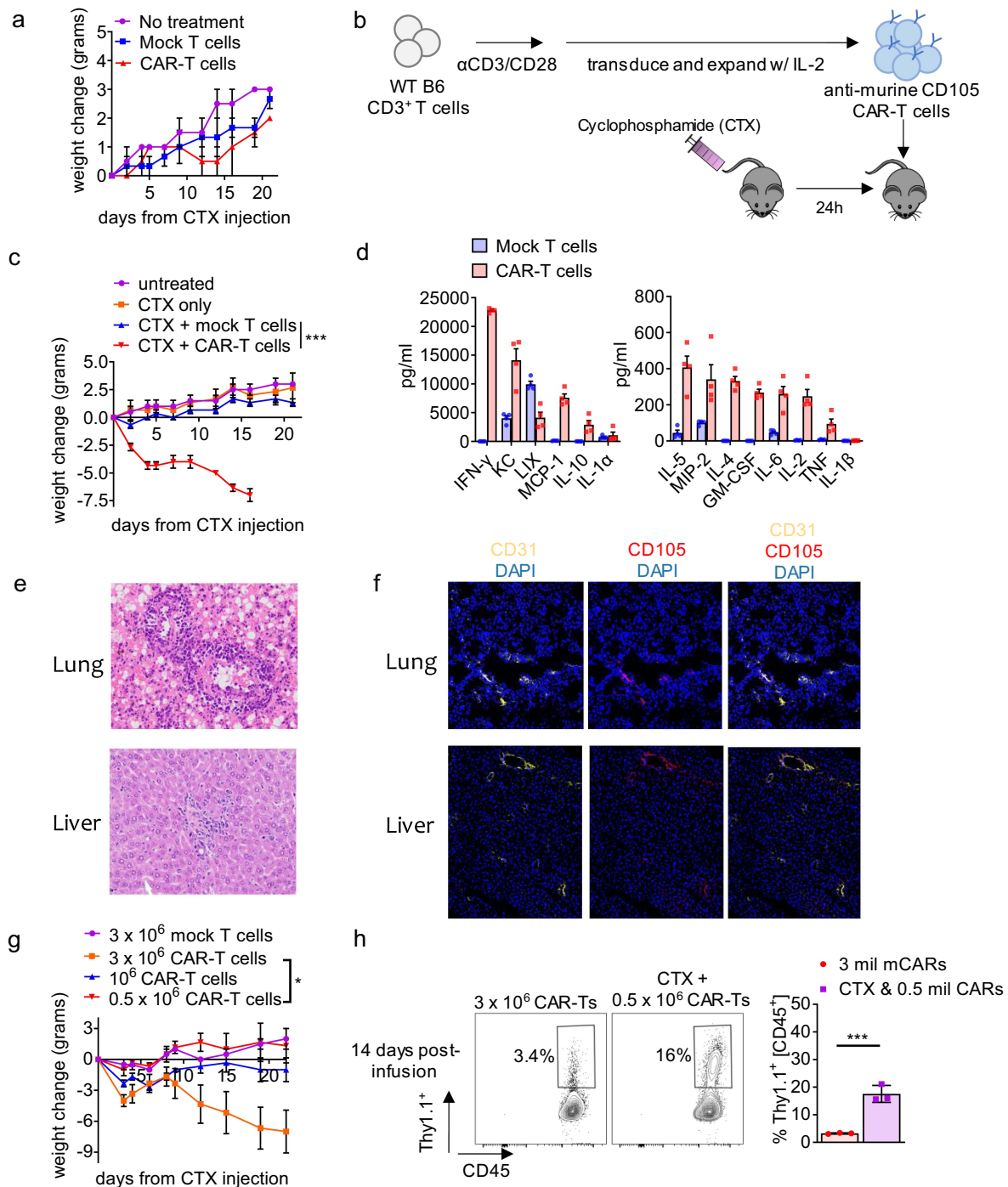


Figure 3. Murine CD105-targeted CAR-T cells exhibit toxicity that is lymphodepletion and dose-dependent. (a) Mouse weight after 3 million murine CAR-T cell infusion (b) Schematic of the lymphodepletion experiment (c) Mouse weight after 3 million murine CAR-T cell infusion with or without 200 mg/kg cyclophosphamide (CTX) conditioning (d) Serum cytokines measured two days after 3 million murine CAR-T cell infusion in cyclophosphamide-conditioned mice (e) Necropsy of mice that were sacrificed because of morbidity (f) Immunofluorescence of lung and liver sections from a healthy mouse (g) Mouse weight after conditioning with 200 mg/kg cyclophosphamide, followed by varying doses of murine CAR-T cells. (h) Engraftment of murine CAR-T cells on day 14 post-infusion. All toxicity experiments (A,C,G) were repeated three times. The cytokine and engraftment data (d,h) are from one cohort. Statistics are repeated-measures ANOVA (c,g) and unpaired t-test (H). * $p < .05$, ** $p < .01$, *** $p < .001$.

Furthermore, central memory CAR-T cells established in the lymph nodes, whereas most CAR-T cells in the tumor were effector memory T cells (Figure 4e). Similar to our findings in the TCR-Tg system,²¹ murine CAR-T cells experienced inability to compete for the glucose tracer 2-NBDG compared to endogenous T cells (Figure 4f) as well as a loss of mitochondrial mass in the tumor microenvironment (Figure 4g).

Murine CAR-T cells both in the tumor and the lymph nodes expressed high levels of inhibitory receptors indicating that either some of the CAR-T cells exhausted in the tumor circulated back to the lymph nodes or were receiving antigenic stimulation in the lymph node microenvironment as well (Figure 5a). This was corroborated with high levels of TOX but also TCF-1⁺ within the CAR-T compartment, a phenotype

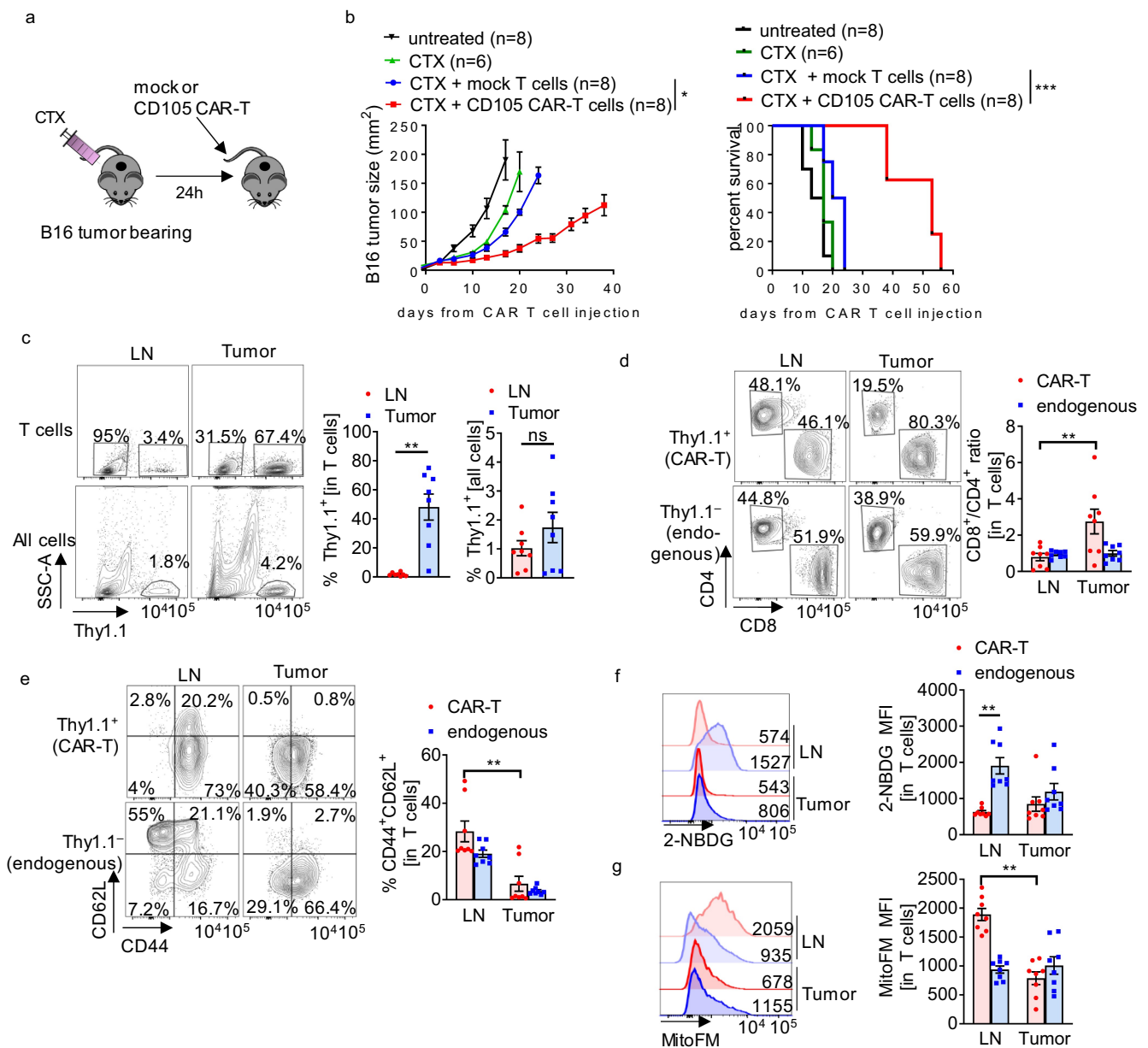


Figure 4. mCD105-targeted CARs are effective in slowing the growth of murine B16 melanoma *in vivo*. (a) Schematic of the therapeutic experiment with murine CAR-T cells against B16 (b) Growth tumor curve and survival of B16-bearing mice treated with 200 mg/kg of cyclophosphamide (CTX) and 0.5 million murine CAR-T cells (c) Distribution of murine CAR-T cells in LN and tumor (d) CD8/CD4 ratio of murine CAR-T cells (CAR-TCs) versus endogenous T cells (ETCs) (e) Memory phenotype of murine CAR-T cells (f) Glucose uptake of murine CAR-T cells (g) Mitochondrial mass of murine CAR-T cells. All experiments were repeated with 3 different donors. All TIL analysis was performed 14 days after cyclophosphamide conditioning & murine CAR-T cell infusion in a design exactly like 4A. For the TIL analysis, the data from the 3 donors were pooled. Statistics are repeated measures ANOVA (B), log-rank test (B) and Wilcoxon matched-pairs signed rank test or paired t-test depending on the data distribution. * $p < .05$, ** $p < .01$, *** $p < .001$.

only existing in the lymph node (Figure 5b). To investigate whether this was happening in non-tumor bearing mice, we analyzed CAR-T cells in the tissue 14 days after infusion. The CAR-T cells exhibited high PD-1 expression but minimal Tim-3 expression, indicating that the presence of the tumor was important for the phenotype of terminal exhaustion observed in the LN (Sup. Figure 1C).

Considering the high level of inhibitory receptors, we proceeded to evaluate function. Despite the high levels of inhibitor receptors, the CAR-T cells were highly proliferative (Figure 5c). In addition, re-stimulation with either PMA/ionomycin or anti-CD3/CD28 led to marked increase in cytokine

production (Figure 5d), suggesting no inherent dysfunction or exhaustion within these cells. However, re-stimulation with CD105 protein showed a significant reduction in cytokine production (Figure 5d) compared to what we observed *in vitro*. (Sup. Figure 1D). To investigate further, we assessed the presence of the CAR on the surface, which we had tagged with the Myc antigen. Although Thy1.1⁺, which marks transduction, was seemingly present in all CAR-T cells, Myc was notably repressed, indicating internalization of the CAR, which was exacerbated in the tumor microenvironment (Figure 5e). We further explored this by activating CAR-T cells *in vitro*, which showed the CAR internalizes rapidly after overnight

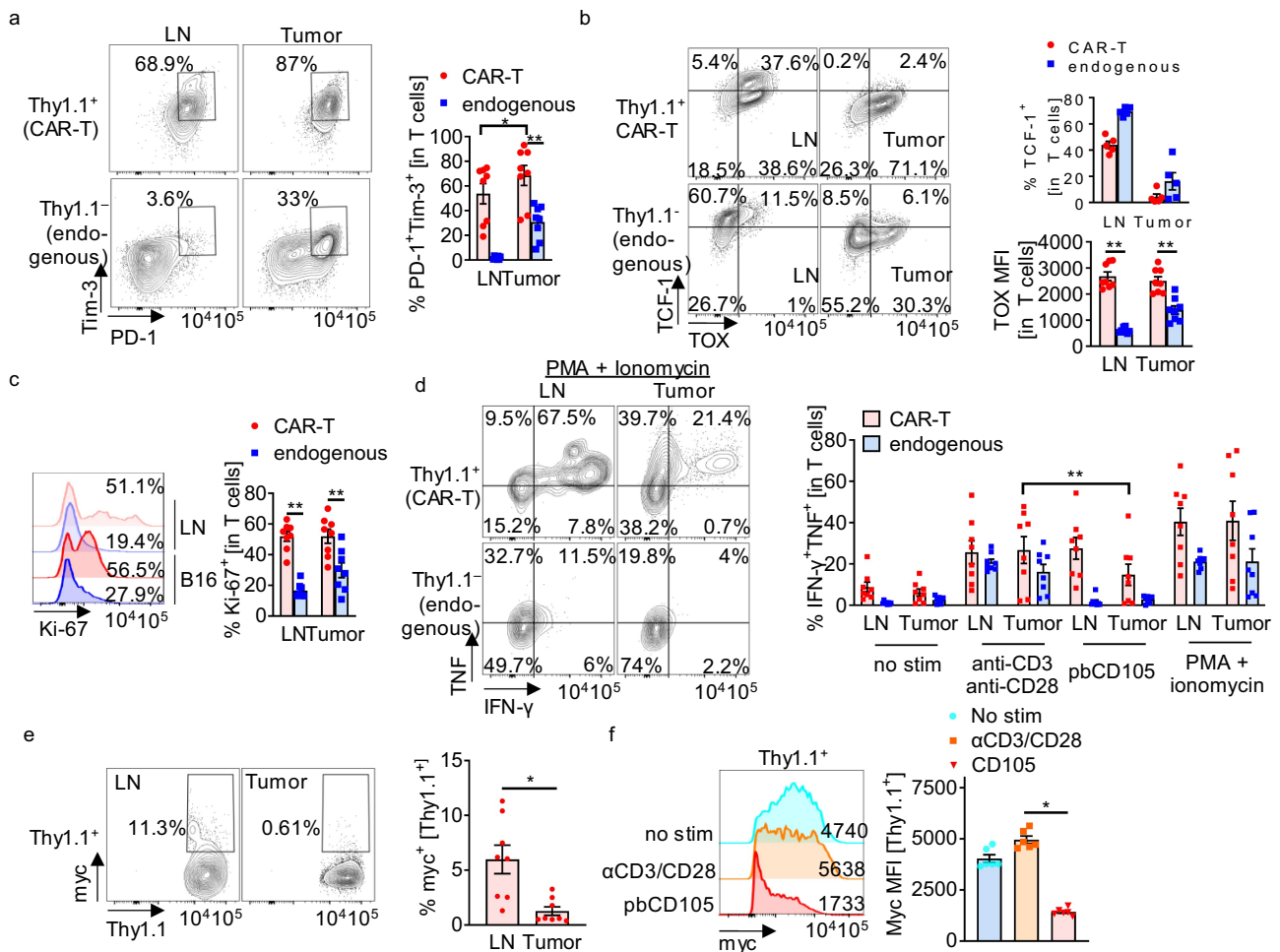


Figure 5. mCD105-targeted CARs are functional despite the expression of inhibitory receptors. (a) Surface exhaustion markers of murine CAR-T cells (b) TCF-1/TOX expression of murine CAR-T cells (c) Ki-67 expression of murine CAR-T cells (d) Cytokine production of murine CAR-T cells after restimulation via TCR, murine CAR or PMA & ionomycin (e) murine CAR surface expression of murine CAR-T cells (f) *In vitro* expression of surface murine CAR after overnight stimulation through the CAR versus the TCR. All experiments were repeated with 3 different donors. All TIL analysis (a-e) was performed 14 days after CTX & murine CAR infusion in a design exactly like 4A. For the TIL analysis, the data from the 3 donors were pooled. Statistics are Wilcoxon matched-pairs signed rank test or paired t-test depending on the data distribution. * $p < .05$, ** $p < .01$.

activation with CD105 but not when activated with anti-CD3 and CD28 (Figure 5f). Indeed, the robust activation of CAR-T cells through their antigen receptor rapidly drove high expression of PD-1 and Tim-3, showing that the expression of these markers is likely evidence of activation and not necessarily exhaustion (Sup. Fig. 1E). Thus overall, cell-intrinsic reasons behind the inability of the cells to clear the tumor during the first 14 days post-infusion are probably due to metabolic deficiencies, which we have shown can impair adoptive cell therapy efficacy, and the downregulation of the CAR itself.^{21,22} Of course, there are many other immunosuppressive factors in the tumor microenvironment that may ultimately impair the function of cell therapies, which we believe this model will help address.

CD105 is a Potential Target of Human CAR-T Cells

The promising results obtained from the murine CAR-T cells led us to consider forward translation toward a human CAR-T product. We assayed human cell lines for CD105 expression, and we found several solid tumor and leukemia cell lines

expressing it apart from the T cell lymphoblastic leukemia Jurkat (Figure 6a). Furthermore, the literature supported that CD105 is frequently expressed in acute myeloid and lymphocytic leukemias as well as in several solid tumors and tumor vasculature.^{18,20} Since CD105 has been targeted before in the clinic with the monoclonal antibody carotuximab with minimal side-effects,²³ we used the binding region of carotuximab to design a human scFv, which we incorporated into a human CAR backbone (Figure 6b). Since the murine CAR was not efficacious *in vivo* with a CD8 hinge domain and there was published evidence that CD8 hinge domains might be interfering with synapse formation we chose a CD28 hinge domain for the human CAR.²⁴ However, we used a 4-1BB co-stimulatory domain as it was shown before in human CAR-T cells that it can increase persistence without a detriment in function.²⁴ Using a retrovirus (MSGV), we transduced peripheral blood mononuclear cells from healthy donors. The transductions were moderate (Sup. Figure 2A), so for most experiments we sorted the cells to achieve purity. The phenotype of the cells at the end of expansion (day 10 from activation) varied among donors but usually the CD4⁺ CAR-T cells outnumbered the

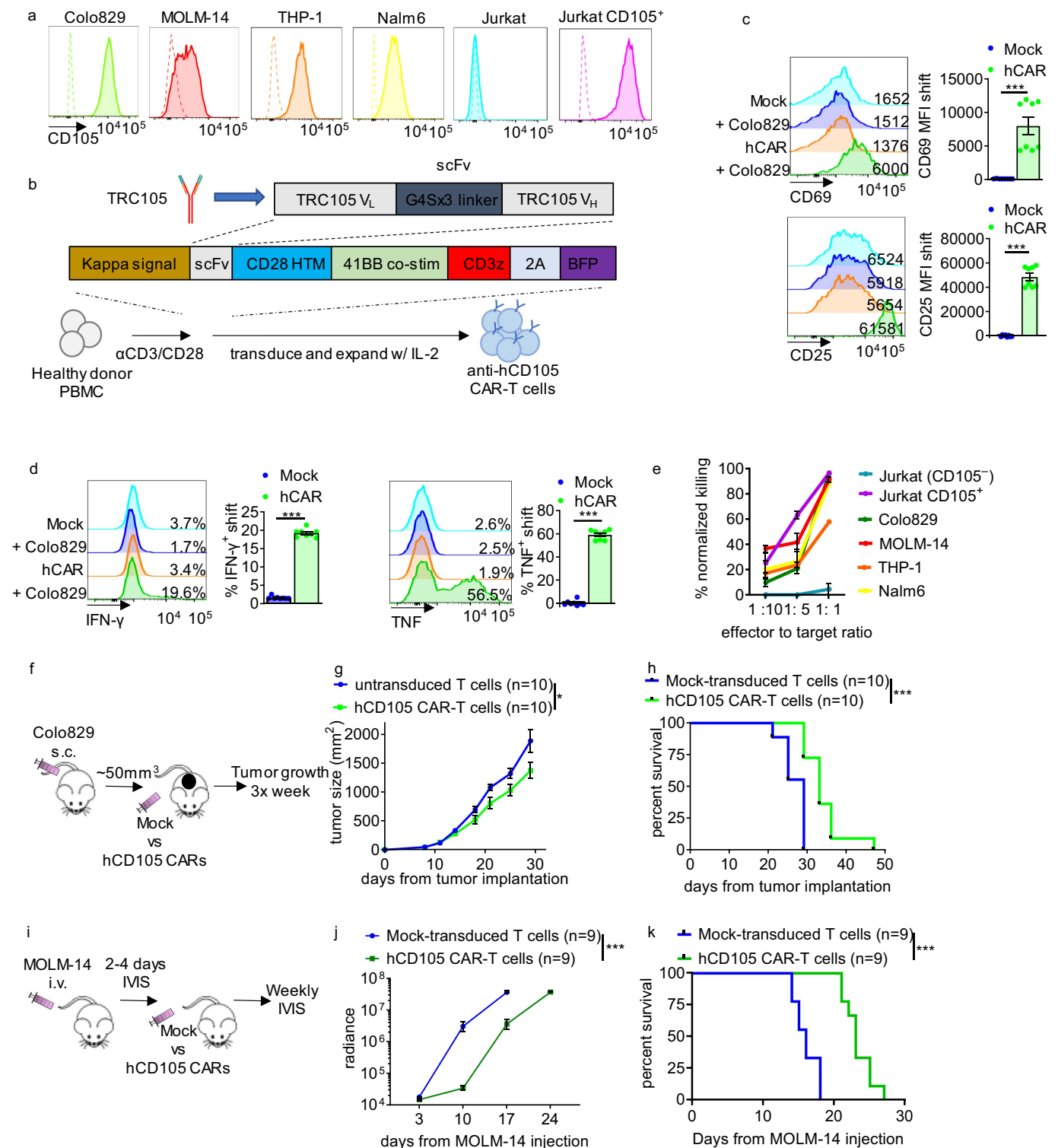


Figure 6. CD105-targeted human CAR T cells exhibit CD105-specific activation and are active in vivo. (a) CD105 expression of human cell lines (b) Engineering of human CD105-targeted CAR from TRC105 (c) Surface activation markers after overnight incubation of human CD105-targeted CAR-T cells with Colo829 at 1:1 ratio (d) Cytokines after 6-hour incubation of human CD105-targeted CAR-T cells with Colo829 at 1:1 ratio (e) Luciferase killing assays after overnight incubation of human CD105-targeted CAR-T cells with target cell lines, normalized to the mock-transduced killing activity. (f) Schematic of the Colo829 *in vivo* experiment (g) Tumor growth curve of Colo829-bearing NSG mice treated with human CAR T cells (h) Survival curve of B (i) schematic of the MOLM-14 *in vivo* experiment (j) Bioluminescence of MOLM-14 engrafted mice treated with human CAR-T cells (k) Survival from E. The activation assays were repeated with 2 different donors and the data were pooled. The killing assays were repeated with 3 different donors. The Colo829 *in vivo* experiment was repeated with 2 different donors and the data were pooled. The MOLM-14 *in vivo* experiment was repeated with 3 different donors and the data were pooled. Statistics are Wilcoxon rank sum test (c,d), repeated measures ANOVA (g, j), log-rank test (h,k). * $p < .05$, ** $p < .01$, *** $p < .001$.

CD8⁺ CAR-T cells and most cells were CD45RO⁺ (Sup. Figure 2b).

We next sought to examine if the human CAR can be activated by the cell lines expressing CD105. We found significant activation (Figure 6c) and cytokine production (Figure 6d) after overnight co-culture with the Colo829 cell line that expresses high levels of CD105. Apart from the activation, the human CD105-targeted CAR-T cells also exhibited efficient killing of cell lines expressing the target (Figure 6e). Importantly, there was no killing against Jurkat cells, but upon overexpression of CD105 via lentivirus, major killing activity was noted. Thus, we decided to investigate whether the human CD105-targeted CAR-T cells can be active *in vivo* against solid and liquid malignancies. NSG mice cohorts bearing either Colo829 melanoma tumors (Figure 6f) or engrafted with MOLM-14 acute myeloid leukemia (Figure 6i), were treated with 10 million human CD105-targeted CAR-T cells or mock-transduced human T cells. The human CAR-T cells slowed the growth of both the melanoma (Figure 6g) and the acute myeloid leukemia (Figure 6j) leading to prolonged survival in both cohorts (Figure 6h and k). These data suggest that not only is CD105 a useful target for understanding the activity of function of CAR-T cells in murine models, but also a potentially important target for human CAR-T cells.

Discussion

Fully murine models of CAR-T cells are scarce despite their significance. We present in this study a fully murine CAR which can target the heavily utilized B16 melanoma model and can be tracked efficiently using congenic markers. Although CD105 CAR-T cells were effective in treating B16 melanoma, they did not eradicate it, which provides a platform to design improvement strategies targeted around various readouts. Importantly, the toxicity observed with this model allows the investigators to concentrate on how to improve the function of the murine CAR-T cells in the tumor microenvironment without worsening the systemic toxicity. In addition, our murine CAR-T cells replicated many biologic phenomena shown previously with either TCR-Tg cells (i.e. loss of mitochondrial mass)²¹ and human CARs (i.e. receptor downregulation).²² Importantly, these murine CAR-T cells can be used on immunocompetent backgrounds, allowing for the study of questions related to the interaction of CAR-T cells with the immune microenvironment. Further, the murine model can also help inform upon the design of strategies that may overcome the need for lymphodepletion, an unfortunate requirement of current cellular therapies.

Previous studies exhibited similar need for lymphodepletion in various murine CAR systems not usually required for TCR-Tg cells.²¹ Kochenderfer et al. showed the murine CD19 CAR-T cells infused after sublethal irradiation could effectively control 38c13 lymphoma¹⁰ whereas Davila et al. showed that murine CD19 CAR-T cells infused after cyclophosphamide treatment could eradicate Eμ-ALL01 leukemia.¹¹ Chinnasamy et al. showed that anti-VEGFR-2 CAR-T cells require lymphodepletion as well to slow down the growth of several tumor lines via targeting their vasculature.¹³ Of note, several degrees of toxicity with murine CAR-T cells have been described before

and they were universally dependent on lymphodepletion.^{12,14,16} In the Moghimi et al. study the toxicity was also dependent on the hinge and co-stimulatory domains used, which was exactly what happened in our model as well.¹⁴ We believe that this is likely secondary to the ineffective CD8 hinge domain rather than the co-stimulatory domain.²⁴

TCR-Tg T cells are frequently used as a model for CAR-T cells in mice, generally as effector T cells expanded *in vitro*. While our data suggest murine CAR-T cells resemble murine TCR-Tg in some respects, there were other features of T cell biology that define the two, most notably that CAR-T cells retained intrinsic functionality during timepoints at which TCR-Tg T cells would be rendered dysfunctional. Our data highlight that care should be taken in equating results obtained with TCR-Tg T cells in cancer therapy to what may be observed in CAR-T cells.

Apart from the murine CD105 CAR-T cell system, we show here that CD105 can also be targeted by human CAR-T cells. CD105 is a promising target for the clinic as it has been targeted with the monoclonal antibody carotuximab with minimal side-effects.²³ Importantly, CD105 is expressed in the activated vasculature of many solid tumors and also in many acute myeloid leukemias, providing several important targets beyond the tumor cell itself.^{18,25} Neither solid tumors nor AML have effective CAR-T cell therapies. CD105 is overexpressed in 30% of AML and has been associated with worse long-term outcomes.^{26,27} Like other antigens in AML, CD105 is not expressed in all blasts; not all blasts have leukemogenic potential. Importantly, Dourado et al showed that for a few patients with CD105-expressing AML blasts, only CD105-positive cells were able to engraft in mice, suggesting that CD105 is a marker of leukemia stem cells in a subset of AML.²⁸ This is further supported by the observation that targeting AML with carotuximab reduced engraftment of AML in mice, indicating that CD105 could be a useful target for the stem-like population in AML. Indeed, human anti-CD105 CAR-T cells prolonged the survival of NSG mice carrying either MOLM-14 AML or Colo829 melanoma. Despite these encouraging results, our CAR-T cell showed moderate activity which could be due to a variety of factors (aggressive cell lines, human donors, low affinity of the CAR to its target antigen) and needs to be further optimized. Of note, recently, another team reported activity of anti-CD105 CARs against hepatocellular carcinoma as well.²⁹

Although carotuximab was safe in clinical trials, there are some concerns about safety for human CD105-targeting CARs. CD105 is expressed in committed erythroid progenitors and the vessels of healing wounds and indeed in the monoclonal antibody trials hypoproliferative anemia and problems with wound healing were encountered.^{23,30,31} Of course, these difficulties are easier to manage than complete bone marrow ablation as a result of CD33 or CD123-targeted CARs.³² Also, the toxicity observed in the mouse, although mitigated with the lower cell dose, raises the concerns for similar phenomena occurring in humans. However, the human protein atlas, did not find any expression of CD105 in the lungs or the liver by immunohistochemistry.³³ They did find though CD105 expression in the kidneys. Kidney injury was not reported as

a common occurrence in the clinical trials with carotuximab though.²³ Notably, the same concern existed with the murine ROR1 CAR, but when nonhuman primates were used to test the potential toxicity for humans, no toxicity was observed.³⁴ A similar avenue could be explored for the human CD105 CAR to ensure safety before considering a phase I trial.

In summary, we have detailed a novel fully murine CAR-T cell system that will support the exploration of many questions in the CAR-T cell field in an immunocompetent setting. The murine CAR-T cells described herein are easy to produce, administer and track *in vivo*. They recapitulate various findings from both TCR-Tg systems and human CARs, indicating that there is a high degree of correlation between the systems and suggests findings with the murine CAR will be likely translatable to other fields. Finally, we showed that CD105 can be targeted with human CARs as well, which are active *in vivo* against human malignancies that have no currently FDA-approved CAR-T cell products.

Materials and methods

Mice

All animal work was done in accordance with the University of Pittsburgh Institutional Animal Care and Use Committee, certified by the Association for Assessment and Accreditation of Laboratory Animal Care. Procedures were performed under their guidelines. C57BL/6 J mice were bred in-house, at a Charles Rivers facility (starting October 2020) or obtained from the Jackson Laboratory. NOD.Cg-Prkdc *scid* Il2rg *tm1Wjl* /SzJ/Arc (NSG) mice were obtained from the Jackson Laboratory.

Cell lines

B16, MOLM-14, THP-1, Nalm6 and Jurkat cell lines were cultured in R10 media (RPMI, 10% FBS, 2 mM L-glut, 100 U/ml PenStrep, 1x NEAA, 1 mM sodium pyruvate, 5 mM HEPES, β -ME). C1498, Plat-E, 293 GP, Colo829 cell lines were cultured in D10 media (DMEM, 10% FBS, 2 mM L-glut, 100 U/ml PenStrep, 1x NEAA, 1 mM sodium pyruvate, 5 mM HEPES, β -ME).

The Colo829 cell lines was originally obtained from ATCC from Dr. Kirkwood who gifted it to our lab. It has not been further authenticated, but it formed appropriate tumors in NSG mice. The MOLM-14/THP-1 cell lines were obtained from Dr Theresa Whiteside. They were not authenticated further but expressed myeloid markers as expected (ie CD33). The THP-1 cell line grew much slower in culture as described already in the literature. The Nalm6 cell lines was a gift from TCR2 therapeutics. It expressed CD19 as expected. Jurkat cells were obtained from Dr Larry Kane who had previously authenticated them by staining with C305, a clonotypic Ab against the Jurkat TCR-beta chain.

Murine CAR-T Cell Generation

Lymph node and spleen T cells were isolated from 6- to 8-week-old C57BL/6 J mice and mechanically disrupted.

T cells were isolated using Biolegend's Mojosort Mouse CD3 T cell isolation kit. The T cells were then activated for 24 hours using plate-bound anti-CD3 (5ug/ml, Biolegend clone 145-2C11), soluble anti-CD28 (2ug/ml, Biolegend clone 37.51) and 50 U/ml murine IL-2 (Peprotech). Prior to the T cell isolation, the viral vectors were transiently transfected into Platinum-E (Plat-E) Retroviral Packaging Cell Line. Retroviral supernatants were harvested, filtered, and flash-frozen at -80°C . After 24 h of murine T cell activation, the viral sups were thawed and 5ug/ml of polybrene was added. Next, the murine T cells were spin-transduced with the retroviral supernatant for 120 min at 2,000 rpm. The cells were left to rest for another 2 hours at 37C in the viral supernatant and then the media was changed to regular R10. The T cells were then expanded with 50 U/ml IL-2 for up to 8 days.

Human CAR-T Cell Generation

X-Vivo 15 media (Lonza) supplemented with 5% human AB serum (Valley Biomedical), 10 mM HEPES buffer and 2 mM GlutaMAX (Gibco) were used for in vitro culture of human CAR-T cells. Frozen PBMCs were thawed and T cells were isolated with the Biolegend Mojosort human CD3 isolation kit. The T cells were then activated with TransAct (Miltenyi Biotec, 1:100) in the presence of 200IU/mL human IL-2 (Cellgenix) for 48 hours, followed by retroviral transduction. Briefly, the retrovirus was pre-loaded through spin-transduction (2 hours, 2000 g) on a non-tissue culture retronectin-coated plate. Then T cells were added and were briefly spun down. The T cells were incubated for 48 hours and then were FACS sorted. After sorting, the T cells were transferred to a G-Rex 6 M Well Plate (Wilson Wolf) for expansion. Cells were then harvested on day 10 for further analysis or adoptive transfer.

Activation Assays

For murine CAR-T cell activations assays, murine CAR-T cells were incubated overnight with plate-bound anti-CD3 (5ug/ml, Biolegend clone 145-2C11) & soluble anti-CD28 (2ug/ml Biolegend clone 37.51) or plate-bound CD105 (2ug/ml, abcam 54339) or PMA (100 ng/ml, Sigma) & Ionomycin (1ug/ml, ThermoFisher). For surface activation markers, the cells were directly stained for flow cytometry in the morning. For cytokines, GolgiPlug (BD, 1:1000) was added in the morning for 6 hours before staining. For activation with target cells, the murine CAR-T cells were co-incubated for the same period of time at a 1:1 ratio with target cells.

For human CAR-T cell activation cytokine assays, human CAR-T cells were incubated with target cells at 1:1 ratio for 6 hours at the presence of GolgiPlug (BD, 1:1000) and then stained for cytokines. For surface activation markers, human CAR-T cells were incubated with target cells at 1:1 ratio overnight and then stained for flow cytometry.

Killing assays

For killing assays, the CAR-T cells were co-cultured with target cells expressing luciferase at different ratios overnight. In the morning, 0.2 mg/ml of luciferin was added to each well and the

luminescence was read by a plate reader. The % killing activity was normalized to the level of signal from the wells that target cells were co-cultured with mock-transduced T cells [%killing = 100*(signal from mock-TD T cell well - signal from CAR-T cell well)/ signal from mock-TD cell well].

In vivo Therapeutic CAR-T Cell Experiments

For murine CAR-T cell experiments, 100k B16 murine melanoma cells were injected intradermally into C57BL/6 J mice. Once tumors became palpable or visible (1–4 mm²), cyclophosphamide 200 mg/kg was injected intraperitoneally. The following day, the mice were randomized based on the tumor sizes. The one group received 0.5 million (unless reported otherwise) murine CAR-T cells intravenously via the retro-orbital approach whereas the other group received mock-transduced T cells. The number of murine CAR-T cells was always adjusted based on % transduction of the product. The tumor growth was monitored 2–3 times per week. A survival event was recorded when tumors ulcerated, surpassed 1.5 cm in diameter or mice died.

For human CAR-T cell experiments with Colo829, 1 million Colo829 cells were injected intradermally into NSG mice. Once tumors reached ~50mm³, the tumors were measured and randomized between two groups. One group received 10 million human CAR-T cells via tail vein injection and the other group received mock-transduced T cells. The tumor growth was monitored 2–3 times per week. A survival event was recorded when tumors ulcerated, surpassed 1.5 cm in diameter or mice died.

For human CAR-T cell experiments with MOLM-14, 0.5 million luciferase-expressing MOLM-14 cells were injected intravenously (through the tail vein) into NSG mice. The mice were then imaged 3 days afterward with IVIS and randomized into two groups. The one group received 10 million human CAR-T cells intravenously via tail vein injection and the other group received mock-transduced T cells. The leukemia burden was monitored with IVIS weekly, whereas morbidity and mortality were monitored daily starting at day 14. A survival event was recorded when mice exhibited morbidity or died.

Tumor-Infiltrating CAR-T Cell Analysis

Lymph nodes and tumors were harvested from C57BL/6 J mice 14 days after murine CAR-T cell transfer. To obtain single-cell suspensions, lymph nodes were mechanically disrupted. Whole tumors were injected using syringes with 2 mg/mL collagenase type IV, 2 U/mL hyaluronidase (Dispase), and 10 U/mL DNase I in serum-free RPMI and incubated for 20 min at 37°C. Tumors were then disrupted and filtered for flow cytometric analysis. Single-cell suspensions were stained and run on BD LSR Fortessa

Flow Sorting and Cytometric Analysis

Staining for murine proteins was performed with anti-mouse specific antibodies obtained from the following companies: Biolegend anti-CD105 (clone MJ7/18), anti-CD4 (clone GK1.5), anti-CD8 (clone 53–6.7), anti-Thy1.1 (clone OX-7),,

anti-PD-1 (clone 29 F.1A12), anti-Tim-3 (clone RMT3-23), anti-CD44 (clone IM7), anti-CD62L (clone MEL-14), anti-CD69 (clone H1.2F3), anti-CD25 (clone PC61), anti-IFN- γ (clone XMG1.2), anti-TNF- α (clone MP6-XT22), anti-IL-2 (clone JES6-5H4), anti-Granzyme B (clone GB11), anti-CD45 (clone 30-F11), anti-Ki67 (clone 16A8). Anti-TOX was purchased from eBioscience (clone TXRX10). Anti-TCF-1 was obtained from Cell Signaling (clone C63D9). Anti-Myc was purchased from Millipore Sigma (clone 4A6). 2-NBDG was obtained from Cayman and Mitotracker Deep Red FM was obtained from Invitrogen.

Staining for human proteins was performed with anti-human specific antibodies obtained from following companies: Biolegend anti-CD4 (clone OKT4), anti-CD8 (clone HIT8a), anti-CD44 (clone BJ18), anti-CD62L (clone DREG-56), anti-CD69 (clone FN50), anti-CD25 (clone M-A251), anti-IFN- γ (clone 4S.B3), anti-TNF- α (clone Mab11), anti-Granzyme B (clone QA16A02). Anti-CD105 was obtained from eBioscience (clone SN6).

Metabolic stains were assayed live. For extracellular only staining, cells were either assayed live or were fixed with 4% PFA. For intracellular staining the cells were first fixed with 4% PFA and then were permeabilized using the FoxP3 fix/perm buffer set (eBioscience) according to the manufacturer's protocol. Intracellular staining was performed overnight at 4°C and buffer was changed in the morning. The cells were then assayed within 1 week from fixation.

Stained cells were analyzed on an LSRFortessa (BD). Cell doublets were excluded by comparison of side-scatter and forward-scatter width to area. Flow-cytometry data were analyzed with FlowJo version 10 software (Tree Star) and figures were produced in Prism version 7 (GraphPad).

Cloning

For the murine CD105-targeted CAR, a scFv was designed based on the binding region of the MJ7/18 antibody. The scFv was then incorporated into a murine CAR-T cell backbone originally designed by Steven Rosenberg's lab (Addgene plasmid 107226) with the exception of the localization signal that was from murine CD8. The MSGV retroviral vector was further modified to carry a myc tag between the CD8 signal and the scFv as well as a Thy1.1 transduction tag which followed the murine CAR after a T2A sequence. 30 μ g of retroviral vector and 10 μ g of pCL-Eco plasmid (Addgene plasmid 12371) were transiently transfected into Platinum-E (Plat-E) Retroviral Packaging Cell Line using Xfect (Takara) for 4 hours. Then media was changed and virus was harvested after 36 hours.

For the human CD105-targeted CAR, a scFv was designed based on the binding region of the carotuximab antibody that has been tested in clinical trials. The scFv was incorporated into a MSGV retroviral human CAR-T cell backbone which was a gift from Jason Lohmueller's lab. 9 μ g of retroviral vector and 4.5 μ g of RD114 plasmid were transiently transfected into 293GP cells using lipofectamine 3000. After overnight incubation the media was changed and the virus was harvested after 24 hours. The 293GP cells and the RD114 plasmid were a gift from Udai Kammula's lab.

All cloning was performed with Hi-Fi DNA Assembly (NEB). Briefly, DNA fragments were produced either with PCR (NEB Q5 master mix and Fisher primers) or with synthetic ds-DNA fragments (gblocks from IDT). The PCR fragments were digested with DpnI (NEB) to remove the original plasmid and were run through a gel to isolate (NEB Monarch DNA Gel extraction kit) the desired band. 25ng of each DNA fragment was added in a reaction with HiFi DNA Assembly and the result of the reaction was transformed into bacteria (NEB C2987H). The colonies were mini-prepped and sent for Sanger Sequencing to Genewiz to confirm the success of the cloning process. The bacteria carrying the desired plasmid were then isolated with NucleoBond Xtra Midi Plus EF from Takara.

Cytokine Measurement

The murine cytokines were measured in mouse blood from the Luminex Core laboratory of the Hillman Cancer Center using the MILLIPLEX MAP Mouse High Sensitivity T Cell Panel – Immunology Multiplex Assay from Millipore Sigma.

Immunofluorescence

Organs were dissected from healthy mice and frozen at -80°C in Optimal Cutting Temperature Compound (Tissue-Tek) and sectioned (Cryostat microtome). Tissue was fixed in histology-grade acetone (Fisher) at -20°C , rehydrated in staining buffer, stained with CD31 Alexa Fluor 647 (clone 390, Biolegend), CD105 Alexa Fluor 594 (clone MJ7/18, Biolegend) and DAPI (Life Technologies), and mounted with ProLong Diamond Antifade Mountant (Life Technologies). All sections were imaged with an Olympus IX83 microscope and analyzed with ImageJ software.

Statistical Analysis

The data presented in the figures are mean \pm standard error of the mean (S.E.M.). For paired data, Wilcoxon matched-pairs signed rank test or paired t-test was used. For unpaired data, Wilcoxon rank-sum test or unpaired t-test was used. The decision about parametric versus non-parametric test was based on visual assessment of the data distribution. Survival data are presented as Kaplan-Meier survival curves and analyzed with the non-parametric log-rank test. Tumor growth curves were analyzed with repeated measures ANOVA. All analysis was completed with Prism v7 software (Graphpad) and confirmed with STATA v17.0. A value of $p < .05$ was considered statistically significant. All tests were two-sided, apart from the tumor growth curves and the survival curve where a one-sided test tested only the hypothesis that the treatment group is better. In the figures, standard designations of significance were given; $*p < .005$, $**p < .01$, $***p < .001$. The specific analysis used per figure in the manuscript can be found within the legends.

Study Approval

All experiments detailed in this manuscript were approved by the University of Pittsburgh Institutional Animal Care and Use

Committee (# 20077737). The use of retroviral vectors was approved by the Institutional Biosafety Committee.

Acknowledgments

This work was supported by TL1 TR001858 to K.L.; an F31 grant (5F31CA257760-02) to A.F.; a National Institutes of Health (NIH) Director's New Innovator Award (DP2AI136598); the Hillman Fellows for Innovative Cancer Research Program; a Stand Up to Cancer–American Association for Cancer Research Innovative Research Grant (SU2C-AACR-IRG-04-16); the Alliance for Cancer Gene Therapy; the UPMC Hillman Cancer Center Skin Cancer and Head and Neck Cancer SPORES (P50CA121973 and P50CA097190; NIH); the Mark Foundation for Cancer Research's Emerging Leader Award; a Cancer Research Institute's Lloyd J. Old STAR Award; and the Sy Holzer Endowed Immunotherapy Fund (all to G.M.D.). The authors would like to thank those in the Luminex Core Laboratory, the Flow Cytometry Core and the Animal Facility of the UPMC Hillman Cancer Center, supported in part by grant P30CA047904 (NIH).

Author contributions

K.L. performed the majority of the experiments and wrote the manuscript. Y.W. performed part of the initial engineering and ruled out many previous murine CAR constructs. M.C. assisted with several *in vivo* experiments. A.K. performed the Colo829 tumor growth curves. S.J. assisted with *in vitro* activation assays. M.P. contributed by measuring tumor growth curves. Y.W. and A.F. assisted with several *in vitro* experiments. J.L. provided guidance on cloning and the design of the vectors. DB. R. implanted tumors for B16 tumor growth curves and provided critical guidance throughout this project. G.M.D. conceived of the study, obtained research funding, oversaw the research, and wrote the manuscript.

Disclosure statement

G.M.D. has filed patent applications around the use of PGC-1 α as a metabolic reprogramming agent in cellular therapies.

Funding

This work was supported by the Cancer Research Institute [Lloyd J. Old STAR Award]; The Mark Foundation for Cancer Research [Emerging Leader Award]; National Institutes of Health [DP2AI136598]; National Institutes of Health [5F31CA257760-02]; National Institutes of Health [TL1 TR001858]; Stand Up To Cancer [SU2C-AACR-IRG-04-16].

Data availability statement

The data will be made available to interested parties after reasonable requests to G.M.D.

References

1. Couzin-Frankel J. Breakthrough of the year 2013. Cancer immunotherapy. *Science*. 2013;342(6165):1432–1433. doi:10.1126/science.342.6165.1432.
2. Ribas A, Wolchok JD. Cancer immunotherapy using checkpoint blockade. *Science*. 2018;359(6382):1350–1355. doi:10.1126/science.aar4060.
3. June CH, Sadelain M. Chimeric antigen receptor therapy. *N Engl J Med*. 2018;379(1):64–73. doi:10.1056/NEJMra1706169.
4. Neelapu SS, Locke FL, Bartlett NL, Lekakis LJ, Miklos DB, Jacobson CA, Braunschweig I, Oluwole OO, Siddiqi T, Lin Y, et al. Axicabtagene ciloleucel CAR T-cell therapy in refractory large b-cell lymphoma. *N Engl J Med*. 2017;377(26):2531–2544. doi:10.1056/NEJMoa1707447

5. Munshi NC, Anderson LD Jr., Shah N, Madduri D, Berdeja J, Lonial S, Raje N, Lin Y, Siegel D, Oriol A, et al. Idecabtagene vicleucel in relapsed and refractory multiple myeloma. *N Engl J Med.* 2021;384(8):705–716. doi:10.1056/NEJMoa2024850
6. Maude SL, Laetsch TW, Buechner J, Rives S, Boyer M, Bittencourt H, Bader P, Verneris MR, Stefanski HE, Myers GD, et al. Tisagenlecleucel in children and young adults with B-cell lymphoblastic leukemia. *N Engl J Med.* 2018;378(5):439–448. doi:10.1056/NEJMoa1709866
7. Shah NN, Lee DW, Yates B, Yuan CM, Shalabi H, Martin S, Wolters PL, Steinberg SM, Baker EH, Delbrook CP, et al. Long-term follow-up of CD19-CAR T-cell therapy in children and young adults with B-ALL. *J Clin Oncol.* 2021;39(15):1650–1659. doi:10.1200/JCO.20.02262
8. Cappell KM, Sherry RM, Yang JC, Goff SL, Vanasse DA, McIntyre L, Rosenberg SA, Kochenderfer JN. Long-term follow-up of anti-CD19 chimeric antigen receptor T-cell therapy. *J Clin Oncol.* 2020;38(32):3805–3815. doi:10.1200/JCO.20.01467
9. Fuca G, Reppel L, Landoni E, Savoldo B, Dotti G. Enhancing chimeric antigen receptor T-cell efficacy in solid tumors. *Clin Cancer Res.* 2020;26(11):2444–2451. doi:10.1158/1078-0432.CCR-19-1835.
10. Kochenderfer JN, Yu Z, Frasher D, Restifo NP, Rosenberg SA. Adoptive transfer of syngeneic T cells transduced with a chimeric antigen receptor that recognizes murine CD19 can eradicate lymphoma and normal B cells. *Blood.* 2010;116(19):3875–3886. doi:10.1182/blood-2010-01-265041.
11. Davila ML, Kloss CC, Gunset G, Sadelain M. CD19 CAR-targeted T cells induce long-term remission and B Cell Aplasia in an immunocompetent mouse model of B cell acute lymphoblastic leukemia. *PLoS One.* 2013;8(4):e61338. doi:10.1371/journal.pone.0061338.
12. Srivastava S, Salter AI, Liggitt D, Yechan-Gunja S, Sarvothama M, Cooper K, Smythe KS, Dudakov JA, Pierce RH, Rader C, et al. Logic-gated ROR1 chimeric antigen receptor expression rescues T cell-mediated toxicity to normal tissues and enables selective tumor targeting. *Cancer Cell.* 2019;35(3):489–503e8. doi:10.1016/j.ccell.2019.02.003
13. Chinnasamy D, Yu Z, Theoret MR, Zhao Y, Shrimali RK, Morgan RA, Feldman SA, Restifo NP, Rosenberg SA. Gene therapy using genetically modified lymphocytes targeting VEGFR-2 inhibits the growth of vascularized syngenic tumors in mice. *J Clin Invest.* 2010;120(11):3953–3968. doi:10.1172/JCI43490
14. Moghimi B, Muthugounder S, Jambon S, Tibbetts R, Hung L, Bassiri H, Hogarty MD, Barrett DM, Shimada H, Asgharzadeh S, et al. Preclinical assessment of the efficacy and specificity of GD2-B7H3 SynNotch CAR-T in metastatic neuroblastoma. *Nat Commun.* 2021;12(1):511. doi:10.1038/s41467-020-20785-x
15. Kato D, Yaguchi T, Iwata T, Katoh Y, Morii K, Tsubota K, Takise Y, Tamiya M, Kamada H, Akiba H, et al. GPC1 specific CAR-T cells eradicate established solid tumor without adverse effects and synergize with anti-PD-1 Ab. *Elife.* 2020;9. doi:10.7554/eLife.49392
16. Wang QJ, Yu Z, Hanada KI, Patel K, Kleiner D, Restifo NP, Yang JC. Preclinical evaluation of chimeric antigen receptors targeting CD70-expressing cancers. *Clin Cancer Res.* 2017;23(9):2267–2276. doi:10.1158/1078-0432.CCR-16-1421
17. Altomonte M, Montagner R, Fonsatti E, Colizzi F, Cattarossi I, Brasoveanu LL, Nicotra MR, Cattelan A, Natali PG, Maio M, et al. Expression and structural features of endoglin (CD105), a transforming growth factor beta1 and beta3 binding protein, in human melanoma. *Br J Cancer.* 1996;74(10):1586–1591. doi:10.1038/bjc.1996.593
18. Cosimato V, Scalia G, Raia M, Gentile L, Cerbone V, Visconte F, Statuto T, Valvano L, D'Auria F, Calice G, et al. Surface endoglin (CD105) expression on acute leukemia blast cells: an extensive flow cytometry study of 1002 patients. *Leuk Lymphoma.* 2018;59(9):2242–2245. doi:10.1080/10428194.2017.1416366
19. Schoonderwoerd MJA, Koops MFM, Angela RA, Koolmoes B, Toitou M, Paauwe M, Barnhoorn MC, Liu Y, Sier CFM, Hardwick JCH, et al. Targeting endoglin-expressing regulatory T cells in the tumor microenvironment enhances the effect of PD1 checkpoint inhibitor immunotherapy. *Clin Cancer Res.* 2020;26(14):3831–3842. doi:10.1158/1078-0432.CCR-19-2889
20. Fonsatti E, Maio M. Highlights on endoglin (CD105): from basic findings towards clinical applications in human cancer. *J Transl Med.* 2004;2(1):18. doi:10.1186/1479-5876-2-18.
21. Scharping NE, Menk AV, Moreci RS, Whetstone RD, Dadey RE, Watkins SC, Ferris RL, Delgoffe GM. The tumor microenvironment represses t cell mitochondrial biogenesis to drive intratumoral T cell metabolic insufficiency and dysfunction. *Immunity.* 2016;45(2):374–388. doi:10.1016/j.immuni.2016.07.009.
22. Li W, Qiu S, Chen J, Jiang S, Chen W, Jiang J, Wang F, Si W, Shu Y, Wei P, et al. Chimeric antigen receptor designed to prevent ubiquitination and downregulation showed durable antitumor efficacy. *Immunity.* 2020;53(2):456–470 e6. doi:10.1016/j.immuni.2020.07.011
23. Rosen LS, Hurwitz HI, Wong MK, Goldman J, Mendelson DS, Figg WD, Spencer S, Adams BJ, Alvarez D, Seon BK, et al. A phase I first-in-human study of TRC105 (Anti-Endoglin Antibody) in patients with advanced cancer. *Clin Cancer Res.* 2012;18(17):4820–4829. doi:10.1158/1078-0432.CCR-12-0098
24. Majzner RG, Rietberg SP, Sotillo E, Dong R, Vachharajani VT, Labanieh L, Myklebust JH, Kadapakkam M, Weber EW, Tousley AM, et al. Tuning the antigen density requirement for CAR T-cell activity. *Cancer Discov.* 2020;10(5):702–723. doi:10.1158/2159-8290.CD-19-0945
25. Schoonderwoerd MJA, Goumans MTH, Endoglin: HL. Beyond the Endothelium. *Biomolecules.* 2020;10(2):289. doi:10.3390/biom10020289.
26. Marklin M, Hagelstein I, Hinterleitner C, Salih HR, Kauer J, Heitmann JS. CD105 (endoglin) as risk marker in AML patients undergoing stem cell transplantation. *Int J Hematol.* 2020;112(1):57–64. doi:10.1007/s12185-020-02875-0.
27. Kauer J, Schwartz K, Tandler C, Hinterleitner C, Roerden M, Jung G, Salih HR, Heitmann JS, Märkl M. CD105 (Endoglin) as negative prognostic factor in AML. *Sci Rep.* 2019;9(1):18337. doi:10.1038/s41598-019-54767-x.
28. Dourado KMC, Baik J, Oliveira VKP, Beltrame M, Yamamoto A, Theuer CP, Figueiredo CAV, Verneris MR, Perlingeiro RCR. Endoglin: a novel target for therapeutic intervention in acute leukemias revealed in xenograft mouse models. *Blood.* 2017;129(18):2526–2536. doi:10.1182/blood-2017-01-763581
29. Mo F, Duan S, Jiang X, Yang X, Hou X, Shi W, Carlos CJJ, Liu A, Yin S, Wang W, et al. Nanobody-based chimeric antigen receptor T cells designed by CRISPR/Cas9 technology for solid tumor immunotherapy. *Signal Transduct Target Ther.* 2021;6(1):80. doi:10.1038/s41392-021-00462-1
30. Dorff TB, Longmate JA, Pal SK, Stadler WM, Fishman MN, Vaishampayan UN, Rao A, Pinski JK, Hu JS, Quinn DI, et al. Bevacizumab alone or in combination with TRC105 for patients with refractory metastatic renal cell cancer. *Cancer.* 2017;123(23):4566–4573. doi:10.1002/ncr.30942
31. Duffy AG, Ma C, Ulahannan SV, Rahma OE, Makarova-Rusher O, Cao L, Yu Y, Kleiner DE, Trepel J, Lee M-J, et al. Phase I and preliminary phase ii study of TRC105 in combination with sorafenib in hepatocellular carcinoma. *Clin Cancer Res.* 2017;23(16):4633–4641. doi:10.1158/1078-0432.CCR-16-3171
32. Mardiana S, Gill SCART. CAR T cells for acute myeloid leukemia: state of the art and future directions. *Front Oncol.* 2020;10:697. doi:10.3389/fonc.2020.00697
33. Accessed March 19, 2022. <https://www.proteinatlas.org/ENSG00000106991-ENG/tissue>
34. Berger C, Sommermeyer D, Hudecek M, Berger M, Balakrishnan A, Paszkiewicz PJ, Kosasih PL, Rader C, Riddell SR. Safety of targeting ROR1 in primates with chimeric antigen receptor-modified T cells. *Cancer Immunol Res.* 2015;3(2):206–216. doi:10.1158/2326-6066.CIR-14-0163.